ORIGINAL ARTICLE

Effect of SiC particles on mechanical properties of multi pass friction stir processed AA7050

Mohd Aqib Khan, Umardaraj Khan

Department of Mechanical Engineering, Vivekananda College of Technology and Management, Aligarh

Abstract

In this work, by implementation of multi-pass friction stir processing (FSP) with SiC nanoparticle was used on AA7050 and encapsulated the joint strength along the different processing parameters of a square pin tool. The impact of multi-pass FSP/SiC nanoparticles on the mechanical properties and microstructure of AA7050 were successfully examined with constant rotational tool speed of 1000 rpm, a traverse speed of 60 mm/min with the tilt angle of 0°. In the stir zone, the microstructure of AA7050 changed to a fine recrystallized grains structure, and SiC nanoparticles were homogeneously distributed in the aluminum metal composite (AMC) due to mechanical stirring. The mechanical property such as hardness was improved by reducing of grain size and dispersed SiC particles. It can be inferred that Nano SiC particles were fragmented totally and uniformly distributed in the 5th pass FSP. Agglomeration of SiC particles decreases with increases in the number of FSP pass. The tensile strength of AA7050 exhibited 310 MPa, and % strain of 16.83. After implementing multi-pass FSP with nanoparticles of SiC on the AA7050, tensile properties were enhanced simultaneously as the FSP pass increases. The maximum tensile strength of one pass, three passes, and five passes was observed as 343.5 MPa, 376.5 MPa, and 441 MPa, respectively.

1. Introduction

Hybrid aluminum matrix nanocomposites (AMNCs) are used in high tech aerospace and automotive to electronic, optical, magnetic and biomedical owing to unique properties as high specific strength, high electrical conductivity, excellent corrosion, and wear resistance [1-3]. Ultrafine grained (UFG) and nanostructured (NS) particulate reinforced hybrid AMNCs have drawn much attention due to their superior physical and mechanical properties in comparison with aluminum alloys [4]. Friction stir processing (FSP) is a novel solid-state workpiece material. Work material is deformed plastically and reinforcing particles mix with base matrix owing to intense

technique for surface modification of metals and alloys based on high temperature severe plastic mixing of the plasticized materials as induced by stirring action of a non-consumable rotating tool [5-7]. Both FSP and FSW work on almost similar principle apart from the fact that while FSP utilizes to process single plate, FSW involves joining of two plates/ workpieces. During FSP, a non-consumable tool (in rotating state) with tailored pin and shoulder design is plunged into base material/workpiece. The stirring action of tool leads to generation of heat of friction between tool and workpiece which in turn results in softening and plasticization of stirring of tool thereby amounting to development of desired composites by FSP [8-10]. This technology has introduced and

employed for various surface treatment applications, such as; elimination of the casting defects, modifying the microstructure of powder metallurgy products, and processing of surface composites [11, 12]. Recently, this FSP route has shown interesting results on the production of ultra-fine grained alloys and metal-matrix nanocomposites due to macro- and micro-scales intermixing of materials aided by the elemental diffusion in Nano-scale [13-15]. New welding approach has been introduced to improve the welding quality of TIG welded joint, the influence of friction stir processing on TIG welded joint have been analyzed and they observed that mechanical properties and heat transfer of TIG+FSP welded joint [16-22]. In the automotive industry, the latest application of FSW is supposedly in the manufacture of a lightweight engine cradle for the 2013 Honda Accord [23]. To offset the strength reduction of FSWed joints, a number of investigators employed heat treatment on 2xxx, 6xxx, and 7xxx aluminum series [24-27]. In this work, the fabrication AMC, FSP was carried out on 7050 aluminum using nano-sized SiC particles to study the influence of nanoparticle and multi-pass FSP on the mechanical properties of the joint.

2. Materials and Method

In present investigation, a 6 mm thick 7050 aluminum plate (chemical composition shown in Table 1) was used. The plate was striped into 150 mm x 40 mm pieces using milling cutter. A groove was machined at the center of the aluminum base sheets with a length, width, and depth of 150, 2.5, and 3 mm, respectively. After inserting SiC nanoparticles inside the groove, a rotating free-pin tool was used to close the surface of the groove for preventing the SiC nanoparticles from throwing out of the groove during FSP. The FSP tool was made from a

heat-treated H-13 tool steel with a hardness of 496HV. Shoulder and pin diameters, pin length, and tilt angle of the square pin tool were 19, 6, 5.5 mm respectively. The traverse and rotation speeds of the tool were kept constant of 1100 rpm, and 60 mm/min respectively. Samples were produced with 1, 3 and 5 passes of FSP. Design expert software is used for the making processing parameters.
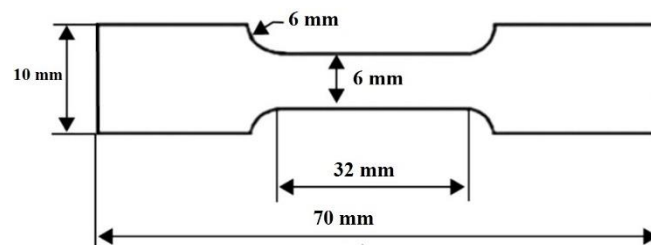

Figure 1: Tensile test specimen as per ASTM E8 standard

In order to investigate the mechanical properties of the multipass FSP/SiC composites, transverse and longitudinal tensile tests and Vickers microhardness test along with the microstructure test were performed. Tensile test specimens were prepared according to the subsize sample of the ASTM E8-M standard with the dimensions shown in Fig. 1. Transverse tensile test was carried out to compare the UTS of the various processed zone (i.e., stir zone, thermo-mechanically affected zone, and heat affected zone) with the base metal. Thus, transverse tensile specimens were extracted from the FSPed samples so that the stir zone was placed at the center of the gage length. Longitudinal tensile test was performed for evaluation of the mechanical behavior of the stir zone, and given this purpose, longitudinal tensile specimens were cut from the center of the stir zone.

Table 1: Chemical composition of AA7050

Material	Si	Cu	Mg	Zn	Fe	Mn	Cr	Ti	Al
AA7050	0.1	2.1	1.8	5.9	0.09	0.06	0.03	0.05	Bal

3. Results and Discussion

3.1 Tensile strength

The effect of processing parameters on microstructure and mechanical properties of the multipass friction stir processing with Nanoparticles SiC have been investigated. Three tensile test specimens for each multipass FSP/SiC samples were tested by a universal testing machine (UTM) as per ASTM E8 standard at room temperature, and average of three have opted. Fig. 2 reveals the stress strain diagram of multi-pass FSP/SiC of Al-7050 at a constant TRS of 1100 rpm, and TS of 60 mm/min. Mechanical properties of each tested specimen i.e. tensile strength, % strain, and hardness were summarized in Table 2. The mechanical properties of FSP samples were mainly controlled by grain size, as long as no reinforcement

particles were used. When reinforcement nanoparticles SiC were included, however, other parameters also contribute to bonding quality between matrix and reinforcements distribution, size, quality of the connection between matrix and the precipitates, reinforcement dispersion pattern, and location generated due to the unequal thermal expansion coefficient of the matrix. [5]. Fig. 2 reveals the stress-strain diagram of AMC subjected to multi-pass FSP/SiC of AA7050. The tensile stress of multi-pass FSP/SiC improved from 328.5 to 441 MPa as the number of passes increased from one to fifth with nanoparticle SiC. The tensile specimens were fractured either TMAZ or HAZ region due to coarse grain structure and minimum hardness. The fracture location in the HAZ and TMAZ were also reported by the past researchers [28].

Table 2: Mechanical Properties of FSPed joint AA7050

Sample No	Nano SiC (%)	No of Pass	Tensile strength (MPa)	Strain (%)	Hardness (HV)	Joint efficiency (%)
1	8.5	3	337.5	14.96	112	108.87
2	12	1	343.5	15.85	108	110.81
3	5	5	426	21.26	128	137.42
4	5	1	388.5	20.52	118	125.32
5	12	3	331.5	16.51	114	106.94
6	5	3	376.5	18.89	119	121.45
7	8.5	1	328.5	16.35	112	105.97
8	12	5	441	22.52	131	142.26
9	8.5	5	406.5	19.52	124	131.13

Because of grains refinement, and equiaxed grain structure of multi-pass FSP/SiC of AA7050, the tensile strength was observed higher than the parent material. The ductility and strength of defect free multi-pass FSP/SiC depends on the base metal's thermal properties [29]. As the number of FSP passes increases, the proof resilience of the multi-pass FSP/SiC was also improved. These results may increase the level of dispersion and fragmentation of SiC nanoparticles and the tendency of the fragmentation of SiC nanoparticles. During axial loading, it resists dislocation movement. The multi-pass FSP persuades intense DRX, dispersion, fragmentation, and material plasticization of SiC with Al-7050 composite.

Figure 2: Stress-strain curve of Al-7050/SiC subjected to multi-pass FSP

Figure 3: Comparison of joint efficiency and grain size of multi-pass FSP/SiC of AA7050

After implementing multi-pass FSP with nanoparticles of SiC on the AA7050, tensile properties were enhanced simultaneously as the FSP pass increases. The maximum joint efficiency and maximum tensile strength was observed 142.26% and 441 MPa at TRS of 1100 rpm, TS of 60 mm/min, with 12% of nanoparticles and fifth pass FSP caused by the formation of strain-free fine grains during DRX and microstructure refinement as shown in fig. 3 and table 2.

3.2 Micro-hardness

Fig. 4 shows that the variation of Vicker hardness to the distance from the weld center of AA7050/SiC aluminum matrix composite (AMC), as the number of passes increases, the hardness values increase. Meanwhile, it may be attributed to the grain fragmentation and refinement of SiC nanoparticles in the AMC. According to the hall-Petch relationship, the occurrence of hard fragmented and reinforcing SiC particles, the refined grain size in the AMC is associated with the thermal input of multi-pass FSP [30, 31]. The three maximum hardness values along the centerline (SZ) were 124, 128, and 131 HV in 5th pass FSP with 8.5, 5, and 12 % of SiC nanoparticles. The base metal AA7050 exhibited a means indentation hardness of 106 HV, while this value-enhanced up to 131 HV in 5th pass FSP with the corporation of a reinforcing agent of SiC nanoparticles. Low fluctuation in hardness in the SZ of all fabricated multi-pass FSP was observed due to dispersion and intermixing of base metal and nanoparticles SiC. The strengthening effect of SiC particles in the five pass FSP was more than one pass FSP due to the hard nature of the SiC phase, fine grains, and material mixing rule.

In multi-pass FSP with filler SiC, the micro-hardness value increased due enhancement of dislocation density, and grain refinement. During multi-pass FSP, intense plastic strain and heat generated by the rotating tool, DRX producing very fine grains leads to the mechanical rapture of inherent grain boundaries. During multi-pass FSP, SiC nanoparticles dispersed in the base metal AA7050 that responsible for grain boundaries. Nanoparticles SiC fragmented during multi-pass FSP does allow grain boundaries to migrate [32]. If the SiC particles are accumulated, it acts as the preferable place for new fine and equiaxed grains after DRX [33]. A very fine grain structure was found by five pass FSP/SiC as compared to the parent metal AA7050, and other FSP passes. So the enhancement of micro-hardness during multi-pass FSP/SiC may be attributed to the combined effect of grain refinement, high hardness of SiC particles, and dispersion strengthening [34].
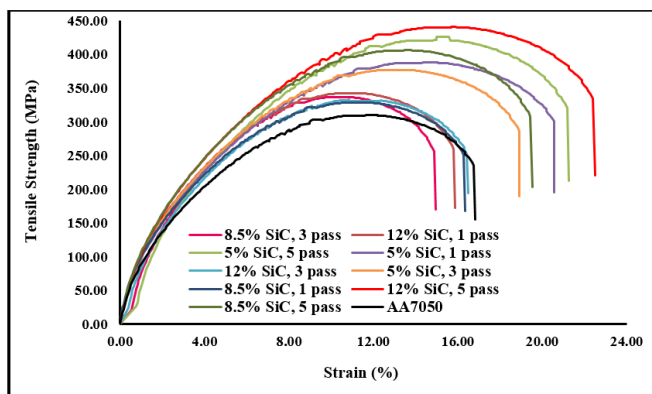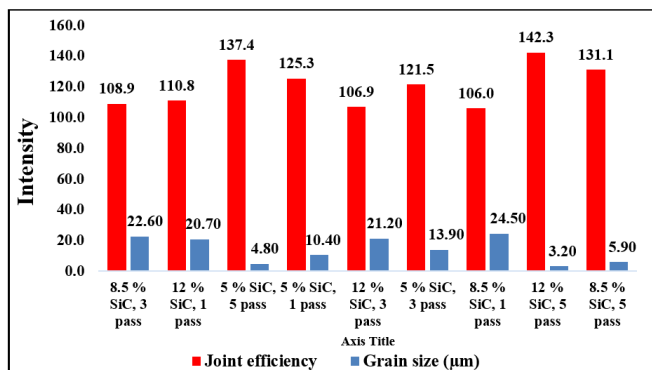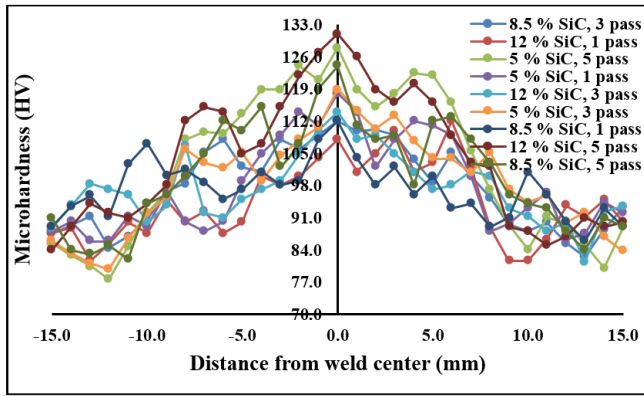
Figure 4: Variation of microhardness of multipass FSP/SiC of AA7050 with different processing parameters

3.3 Microstructure analysis

Fig. 5 reveals the microstructure of one pass FSP/SiC, three pass FSP/SiC, and five pass FSP/SiC. The samples of microstructure were polished by the emery papers from grit size 400 to 2200, and final polishing was done by alumina powder by the disc polishing machine. After polishing, the specimens were dip in to killer reagent (6ml of HCL, 8ml of HNO_3 and 4ml of HF) as per ASTM E407 standard. Due to adequate softening of the material, the uniform distribution of fine grains in the SZ were observed and reveals the maximum hardness and tensile strength of the multi-pass FSP [35].

Fig.5a illustrated the optical microstructure of 1 pass FSP of AA7050 observed fine grains structure of an average grain size of 20.7± 5 μm. The severe plastic deformation, and dynamic recrystallization was induced by tool stirring action of one pass FSP, the microstructure of AA7050 was considerably refining in the region SZ, TMAZ, and HAZ. The average grain size of base metal and multi-pass FSP samples was analyzed by image J software, and found grain size of one pass, three passes, and five passes was 20.7 μm, 13.9 μm, 3.2 μm, respectively as shown in fig. 6.

Figure 5: Optical microstructure of multipass FSP/SiC, (b) 1 pass FSP, (c) 3 pass FSP, (d) 5 pass FSP

In one pass FSP, the modified grain structural refinement of AA7050 towards SZ, TMAZ, and HAZ was changed gradually. Nanoparticles of SiC was introduced for further refinement in the SZ during one, three, and fifth passes of FSP as presented in fig. 5. A sharp grain structure was found from the parent metal to HAZ, TMAZ, and SZ, and observed fine and equiaxed nanoparticles inside the TMAZ and SZ as compared to the base metal. A microstructural modification was convinced during hybrid multi-pass FSP/SiC Nanocomposite. The SZ develops a degree of refinement, fine and equiaxed recrystallized grains that depend on the temperature gradient across the SZ, which may change particle distribution and refinement and the grain structure through the thickness direction [36].

3.4 Fracture analysis

The fracture analysis of multi-pass FSP/SiC was done by SEM machine and observed the failure pattern, tiny and ductile dimples on the multi-pass FSP samples. The higher area of tiny and ductile dimples and least amount of cleavage facets was observed in the five pass FSP/SiC. Fig. 7a-b depicts the fracture surfaces of the composite AA7050/SiC with one pass and five pass FSP. The shear plane of 45º to the tensile axis was formed along the periphery of the specimens during the tensile test, forming a cup-cone fracture [37, 38]. The tiny and

equiaxed dimples were observed in five pass FSP/SiC fractured sample which indicating ductile failure. One pass FSP/SiC specimen showed the honey comb dimples which shows microporous and agglomerative ductile fractures. The microstructure of the composite AA7050/SiC with fifth passes showed uniform and finer than the other passes, and it was also reveals from the fracture morphology that the dimple size in multi-pass FSP/SiC was smaller than the parent metal AA7050; that's why the mechanical properties of multi-pass FSP/SiC was much higher than the base metal AA7050.
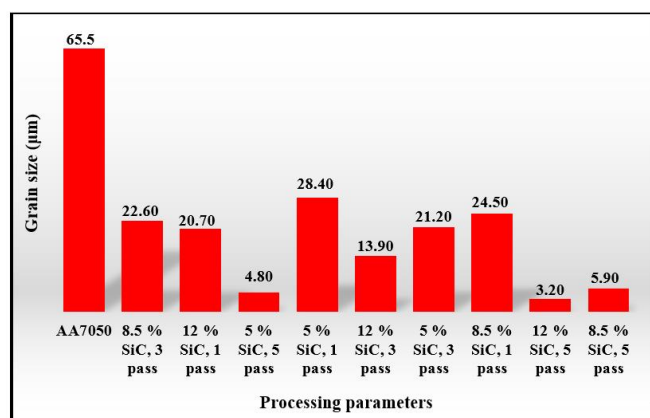

Figure 6: Comparison of grain size to the processing parameters of multipass FSP/SiC of AA7050

The ductile fracture with honeycomb dimples were observed in one pass FSP/SiC, and the separated features on the fracture surface showed characteristics of both plastic deformation and cleavage [39]. All multi-pass FSP samples processed at a constant TRS and TS. During the multi-pass FSP/SiC, the uniform dispersion of reinforcement particles, consequently decreasing the grain size, effectual material mixing, fine and equiaxed dimples, were observed. All the multi-pass FSP/SiC samples were fractured in the HAZ or TMAZ region due to coarse grains structure and material softening as confirmed by variation in the microhardness [40].

3.5 Conclusions

The impact of multi-pass FSP/SiC nanoparticles on the mechanical properties and microstructure of AA7050 were successfully examined with constant rotational tool speed of 1000 rpm, a TS of 60 mm/min with the TTA of 0º. The results can be summarized as follow.

- In the SZ, the microstructure of AA7050 changed to a fine recrystallized grains structure, and SiC nanoparticles were homogeneously distributed in the AMC due to mechanical stirring. The mechanical property such as hardness was improved by reducing of grain size and dispersed SiC particles.
- It can be inferred that Nano SiC particles were fragmented totally and uniformly distributed in the 5th pass FSP. Agglomeration of SiC particles decreases with increases in the number of FSP pass.
- The tensile strength of AA7050 exhibited 310 MPa, and % strain of 16.83. After implementing multi-pass FSP

with nanoparticles of SiC on the AA7050, tensile properties were enhanced simultaneously as the FSP pass increases. The maximum tensile strength of 1 pass, three passes, and 5 passes was observed as 343.5 MPa, 376.5 MPa, and 441 MPa, respectively.

- Vickers's hardness value along the centerline (SZ) was observed as 118, 119, and 131 HV with 1, 3, and 5 FSP pass, respectively.
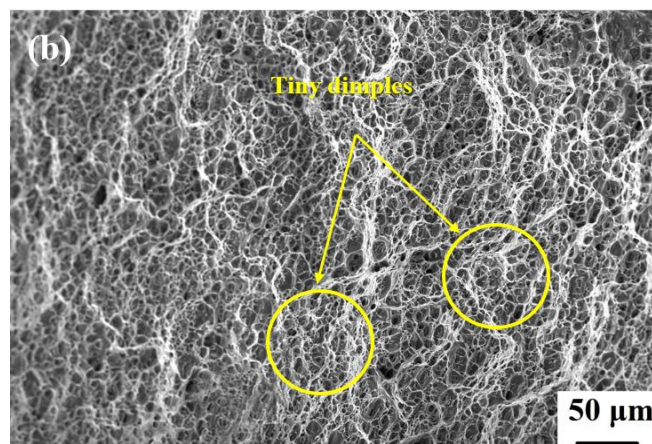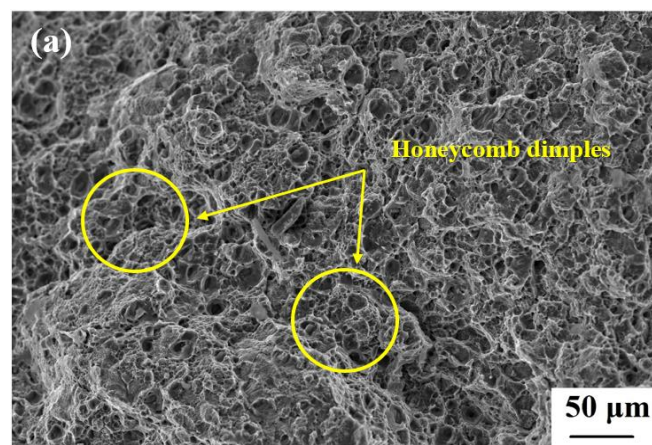

Figure 7: Fractography of AA7050/SiC composite, (a) one pass, (b) five passes

References

[1] N. Gangil, A.N. Siddiquee, S. Maheshwari, Aluminium based in-situ composite fabrication through friction stir processing: a review, J. Alloys Compd. 715 (2017) 91–104.

[2] Husain Mehdi, R.S. Mishra, Analysis of Material Flow and Heat Transfer in Reverse Dual Rotation Friction Stir Welding: A Review, International Journal of Steel Structure, 19, 422–434 (2019).

[3] V. Sharma, U. Prakash, B.V.M. Kumar, Surface composites by friction stir processing: a review, J. Mater. Process. Technol. 224 (2015) 117–134

[4] M.I.A. El Aal, H.S. Kim, Wear properties of high pressure torsion processed ultrafine grained Al-7%Si alloy, Mater. Des. 53 (2014) 373–382,

[5] R.S. Mishra, Z.Y. Ma, Friction stir welding and processing, Mater. Sci. Eng. R 50 (1–2) (2005) 1–78,.

[6] F. Khodabakhshi, B. Marzbanrad, L.H. Shah, H. Jahed, A.P. Gerlich, Friction-stir processing of a cold sprayed AA7075 coating layer on the AZ31B substrate: structural homogeneity, microstructures and hardness, Surf. Coat. Technol. 331 (Supplement C) (2017) 116–128,

[7] F. Khodabakhshi, A.P. Gerlich, Potentials and strategies of solid-state additive friction-stir manufacturing technology: a critical review, J. Manuf. Process. 36 (2018) 77–92.

[8] Rathee S, Maheshwari S, Noor Siddiquee A (2018) Issues and strategies in composite fabrication via friction stir processing: A review. Mater Manuf Process 33(3):239–261.

[9] Husain Mehdi, R.S. Mishra, Study of the influence of friction stir processing on tungsten inert gas welding of different aluminum alloy, SN Applied Sciences 1. (2019) 1: 712.

[10] Husain Mehdi, R.S Mishra, Mechanical Properties and Microstructure Studies in Friction Stir Welding (FSW) Joints of Dissimilar Alloy A Review, Journal of Achievements of Materials and Manufacturing Engineering (Scopus), vol 77, issue 1, 2016.

[11] Z.Y. Ma, Friction stir processing technology: a review, Metall. Mater. Trans. A 39 (3) (2008) 642–658,

[12] F. Khodabakhshi, H. Ghasemi Yazdabadi, A.H. Kokabi, A. Simchi, Friction stir welding of a P/M Al-Al 2 O nanocomposite: microstructure and mechanical properties, Mater. Sci. Eng. A 585 (2013) 222–232,

[13] R.S. Mishra, Z.Y. Ma, I. Charit, Friction stir processing: a novel technique for fabrication of surface composite, Mater. Sci. Eng. A 341 (1–2) (2003) 307–310,

[14] F. Khodabakhshi, A.P. Gerlich, A. Simchi, A.H. Kokabi, Cryogenic friction-stir processing of ultrafine-grained Al-Mg-TiO nanocomposites, Mater. Sci. Eng. A 620 (2014) 471–482.

[15] F. Khodabakhshi, A. Simchi, A.H. Kokabi, A.P. Gerlich, M. Nosko, Effects of stored strain energy on restoration mechanisms and texture components in an aluminum–magnesium alloy prepared by friction stir processing, Mater. Sci. Eng. A 642 (2015) 204–214.

[16] Husain Mehdi, R.S.Mishra, Microstructure and mechanical characterization of TIG-welded joint of AA6061 and AA7075 by friction stir processing, Part L: Journal of Materials: Design and Applications, May 2021. DOI: 10.1177/14644207211007882

[17] Husain Mehdi, R.S. Mishra, Effect of Friction Stir Processing on Mechanical Properties and Wear Resistance of Tungsten Inert Gas Welded Joint of Dissimilar Aluminum Alloys. Journal of Material Engineering and Performance 30, 1926–1937 (2021).

[18] Husain Mehdi, R.S. Mishra, Influence of friction stir processing on weld temperature distribution and mechanical properties of TIG welded joint of AA6061 and AA7075, Transactions of the Indian Institute of Metals, 73, 1773–1788 (2020).

[19] Husain Mehdi, R.S. Mishra, Effect of friction stir processing on mechanical properties and heat transfer of TIG-welded joint of AA6061 and AA7075, Defence Technology (2020).

[20] Husain Mehdi, R.S. Mishra, Effect of Friction Stir Processing on Microstructure and Mechanical Properties of TIG Welded Joint of AA6061 and AA7075, Metallography, Microstructure, and Analysis, 9, 403–418 (2020).

[21] Husain Mehdi, R.S. Mishra, Investigation of mechanical properties and heat transfer of welded joint of AA6061 and AA7075 using TIG+FSP welding approach, Journal of Advanced Joining Processes, 1,100003, (2020).

[22] Husain Mehdi & R.S. Mishra (2020) An experimental analysis and optimization of process parameters of AA6061 and AA7075 welded joint by TIG+FSP welding using RSM, Advances in Materials and Processing Technologies, DOI: 10.1080/2374068X.2020.1829952

[23] Gibson BT, Lammlein DH, Prater TJ, Longhurst WR, Cox CD, Ballun MC, et al. Friction stir welding: process, automation, and control. J Manuf Process 2014;16:56–73.

[24] Elangovan K, Balasubramanian V. Influences of post-weld heat treatment on tensile properties of friction stir-welded AA6061 aluminum alloy joints. Mater Charact 2008;59:1168–77.

[25] Aydın H, Bayram A, Durgun ˙ I. The effect of post-weld heat treatment on the mechanical properties of 2024-T4 friction stir-welded joints. Mater Des 2010;31:2568–77,

[26] Sharma C, Dwivedi DK, Kumar P. Effect of post weld heat treatments on microstructure and mechanical properties of friction stir welded joints of Al–Zn–Mg alloy AA7039. Mater Des 2013;43:134–43.

[27] Sun YF, Fujii H. The effect of SiC particles on the microstructure and mechanical properties of friction stir welded pure copper joints. Mater Sci Eng A 2011;528:5470–5 .

[28] M. Koilraj, V. Sundareswaran, S. Vijayan , S.R.K. Rao, Friction stir welding of dissimilar Al-alloys AA2219 to AA5083- Optimization of process parameters using Taguchi technique. Materals and Design, 2012, **42**, 1–7.

[29] O.T. Middling, L.D. Oosterkamp, J. Bersaas, Friction stir welding aluminium process and applications. Int: Proc.7 Inter. conf. jt. alum., 1998, INALCO98.

[30] S.S. Mirjavadi, M. Alipour, A.M.S. Hamouda, A. Matin, S. Kord, B.M. Afshari, P.G. Koppad, Effect of multi-pass friction stir processing on the microstructure, mechanical and wear properties of AA5083/ZrO_2 nanocomposites, J. Alloys Compd. 726 (2017) 1262–1273.

[31] V. Ebrahimzadeh, M. Paidar, M.A. Safarkhanian, O.O. Ojo, Orbital friction stir lap welding of AA5456-H321/AA5456-O Al-alloys under varied parameters, Int. J. Adv. Manuf. Technol. 96 (2018) 1237–1254.

[32] H.A. Deore , A. Bhardwaj, A.G. Rao, J. Mishra, V.D. Hiwarkar, Consequence of reinforced SiC particles and post process artificial ageing on microstructure and mechanical properties of friction stir processed AA7075, Defence Technology 16 (2020) 1039-1050.

[33] M. Bodaghi, K. Dehghani, Friction stir welding of AA5052: the effects of SiC nanoparticles addition, Int. J. Adv. Manuf. Technol. 88 (2017) 2651–2660.

[34] Fuller CB, Mahoney MW, Calabrese M, Micona L. Evolution of microstructure and mechanical properties in naturally aged 7050 and 7075 Al friction stir welds. Mater Sci Eng A 2010;527(9):2233-2240.

[35] H. Mohammadzadeh Jamalian, M. Farahani, M. K. Besharati Givi, and M. Aghaei 8 Vafaei (2016), "Study on the effects of friction stir welding process parameters on the microstructure and mechanical properties of 5086-H34 aluminum welded joints," International Journal of advanced manufacturing technology, vol. 83, no. 1–4, pp. 611–621.

[36] A. Sharma, V.M. Sharma, S. Mewar, S.K. Pal, J. Paul, Friction stir processing of Al6061-SiC-graphite hybrid surface composites, Mater. Manuf. Process. 33 (7) (2018) 795–804.

[37] C.Pandey, N. Saini, M.M. Mahapatra, P. Kumar, Study of the fracture surface morphology of impact and tensile tested cast and forged (C&F) Grade 91 steel at room temperature for different heat treatment regimes, Eng. Fail. Analy, 2017, **71**, p131-147.

[38] Nitin Saini, Chandan Pandey, Manas Mohan Mahapatra, H.K.Narang, R.S.Mulik, Pradeep Kumar, A comparative study of ductile-brittle transition behavior and fractography of P91 and P92 steel, Engineering Failure Analysis, 81, 2017, 245-253.

[39] Akbar Heidarzadeh, Reza Vatankhah Barenji, Mohsen Esmaily, Atabak Rahimzadeh Ilkhichi, Tensile Properties of Friction Stir Welds of AA 7020 Al-alloy, Trans Indian Inst Met, 2015, **68**, p757–767.

[40] R.I. Rodriguez, J.B. Jordon, P.G. Allison, T. Rushing, L. Garcia, Microstructure and mechanical properties of dissimilar friction stir welding of 6061-to-7050 Al-alloys, Mat. Des., 2015, **83**, p60–65.